$$s_m = \frac{MRI}{n_j + \frac{Mn_s}{K'}} \tag{20}$$

where R is the output resistance of the phototube, n_j is the Johnson noise, independent of cathode current I, and n_s is the shot noise proportional to $\sqrt{I}$. $1/K'$ is, as before, a factor representing the increase in noise in a multiplier phototube due to various minor factors such as shot noise at the dynodes and nonuniform multiplication across the cathodes' surface.

Clearly, the break-even point occurs when

$$Mn_j + Mn_s = n_j + \frac{1}{K'}Mn_s$$

or

$$\frac{n_j}{n_s} = \frac{\frac{1}{K'} - 1}{1 - \frac{1}{M}} \doteq \frac{1}{K'} - 1 \tag{21}$$

If it is again assumed that $K' = 0.5$, the break-even point occurs when $n_j = n_s$. But $n_j^2 = 4kTR\Delta f$ and $n_s^2 = 2R^2eI\Delta f$, so that the foregoing requirement reduces to

$$\frac{2kT}{eR} = I = \sigma L$$

or

$$L = \frac{2kT}{\sigma eR} = 5.14 \times 10^5 / R\sigma \text{ lumen} \tag{22}$$

at room temperature, where $T = 300$ (Boltzmann's constant $k = 1.37 \times 10^{-16}$ and $e = 1.6 \times 10^{-19}$).

The maximum value of R will, of course, be determined by the interelectrode capacitances of the phototube and the bandwidth requirement.

If the design is limited to $R = \frac{1}{2\pi fC}$, equation 22 reduces to

$$L = 3.23 \times 10^6 fC/\sigma \tag{23}$$

This result shows that in all practical cases a multiplier phototube will provide the higher signal-to-noise ratio as long as its anode ratings permit it to be operated with appreciable multiplication.

References

1. Calculated Frequency Spectrum of the Shot Noise from a Photo-Multiplier Tube, **R. D. Sard.** *Journal of Applied Physics*, New York, N. Y., vol. 17, 1946, pp. 768–77.

2. Vacuum Tube Amplifiers. *Radiation Laboratory Series*, Massachusetts Institute of Technology, Cambridge, Mass., McGraw-Hill Book Company, Inc., New York, N. Y., vol. 18, 1948, Rule 4, p. 80.

3. *Ibid.*, Rule 1, p. 77.

4. Multiplier Phototube Characteristics: Application to Low Light Levels, **R. W. Engstrom.** *Journal of the Optical Society of America*, New York, N. Y., vol. 37, 1947, pp. 420–31 (extensive bibliography).

5. The Secondary Emission Multiplier, **V. K. Zworykin, G. A. Morton, L. Malter.** *Proceedings*, Institute of Radio Engineers, New York, N. Y., vol. 24, 1936, pp. 351–75.

6. A Theory of Noise for Electron Multipliers, **W. Shockley, J. R. Pierce.** *Ibid.*, vol. 26, 1938, pp. 321–32.

7. Photoelectric Multipliers, **S. Rodda.** *Journal of Scientific Instruments and of Physics in Industry*, London, England, vol. 26, 1949, pp. 65–70.

8. The Principles of Optics, **Hardy and Perrin.** McGraw-Hill Book Company, Inc., New York, N. Y., 1932, equation 223, p. 411.

Impedance of Thin-Wire Loop Antennas

JAMES E. STORER
NONMEMBER AIEE

THE THIN-wire loop is one of the first antennas to receive theoretical consideration, having been discussed by Pocklington[1] in 1897. Pocklington treated a closed loop excited by a plane wave; he obtained an exact solution for the current on the loop in the form of a Fourier series. More recently, Hallén[2] considered a driven loop and obtained a solution, again in the form of a Fourier series, for the current and the impedance. However, Hallén pointed out that the coefficients of this series contained a singularity which made the series only quasiconvergent and hence useful only for loops small in comparison to a wave length. Moreover, the individual terms were complicated and their evaluation and a summation involved a somewhat difficult numerical task.

More recently, in an effort to obtain numerical results, other authors have dealt with the problem using approximation methods. Chang,[3] for example, applied the Hallén-King-Middleton expansion; Schelkunoff[4] has used a guided mode approximation; and the author has used a variational approach (unpublished). All of these approximation methods have one feature in common; they yield results which are in good agreement qualitatively with experiment, but poor agreement quantitatively. (It is quite possible that all of these methods, particularly Chang's could be made to yield better results by going to higher degrees of approximation; the resulting numerical labor, however, is likely to be prohibitive.) The reason for this can be explained by noting that all the approximation methods require some assumption as to the current distribution around the loop. The most common assumption is that the current distribution approximates a sinusoidal distribution. As will be shown subsequently, the sinusoidal assumption is not satisfactory, particularly for the current near the driving point of the antenna.

In this paper the rigorous Fourier series solution obtained by Hallén is reexamined, and modified so that the convergence difficulties which he encountered are avoided. Extensive numerical results are presented in Appendix I for the impedances of loops for varying wire sizes and circumferences up to $2^1/_2$ wave lengths. Appendix II presents some curves which aid in the computation of field patterns and current distributions. For an antenna having a particular wire size, some experimentally measured impedances are presented which agree well with theory.

Fourier Series Solution for the Current Distribution

Integral equations for the current distribution on thin-wire antenna structures are readily obtained by expressing the electric field as a function of the current, through Helmholtz integrals, and then equating the total electric field to zero along the wire surface. Following this procedure, with harmonic time dependence of the form $\epsilon^{+j\omega t}$, and with co-ordinate system and dimensions as indicated in Fig. 1, the integral equation for the circular loop antenna can be written as

$$V\delta(\phi) = \frac{j\zeta_0}{4\pi}\int_{-\pi}^{\pi} K(\phi - \phi')I(\phi')d\phi' \tag{1}$$

where $I(\phi)$ is the total current at ϕ on the loop; V is the voltage of the slice generator exciting the loop at $\phi = 0$; $\delta(\phi)$ is the

Paper **56-692**, recommended by the AIEE Special Communications Applications Committee and approved by the AIEE Committee on Technical Operations for presentation at the AIEE Summer and Pacific General Meeting, San Francisco, Calif., June 25–29, 1956. Manuscript submitted October 28, 1955; made available for printing June 6, 1956.

Dr. James E. Storer is with Harvard University, Cambridge, Mass.

The author wishes to thank Prof. R. W. P. King of Harvard University for his help and encouragement with this research; Miss Phyllis Kennedy for making her experimental measurements available; and to Leon Levy, who performed the numerical computations. The author also wishes to acknowledge the financial support he received from the Atomic Energy Commission as a Fellow during the early phase of this research; and during the latter part, under the sponsorship of the Office of Naval Research, the Signal Corps of the U. S. Army, and the U. S. Air Force *Contract N5ori-76*. This research was originally published as *Technical Report No. 212*, Cruft Laboratory, Harvard University, May 1, 1955.

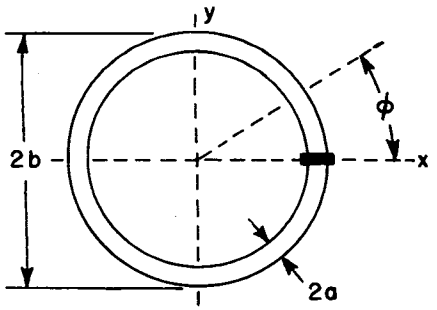

Fig. 1. Co-ordinates for loop antenna

Dirac delta function; and $k=\omega/c=2\pi/\lambda$; $\zeta_0=\sqrt{\frac{\mu_0}{\epsilon_0}}=120\pi$ ohms. The kernel of the integral equation 1 is given explicitly by

$$K(\phi-\phi')=\left[kb\cos(\phi-\phi')+\frac{1}{kb}\frac{\partial^2}{\partial\phi^2}\right]\times\frac{\epsilon^{-jkbR(\phi-\phi')}}{R(\phi-\phi')} \quad (2A)$$

$$R(\phi-\phi')=\left[4\sin^2\left(\frac{\phi-\phi'}{2}\right)+a^2/b^2\right]^{1/2} \quad (2B)$$

where a is the radius of the wire and b is the radius of the loop.

The thin-wire assumption, which provides the basis for obtaining this one-dimensional current equation, can be expressed explicitly as $a^2<<b^2$, $k^2a^2<<1$. The resulting solution cannot be more accurate than the order of these approximations.

Since $\frac{1}{R(\phi-\phi')}\epsilon^{-jkbR(\phi-\phi')}$ is a bounded, periodic function of ϕ, it can be expanded into a Fourier series, i.e.

$$\frac{1}{R(\phi-\phi')}\epsilon^{-jkbR(\phi-\phi')}=\sum_{-\infty}^{\infty}K_n\epsilon^{-jn(\phi-\phi')} \quad (3)$$

$$K_n=K_{-n}=\frac{1}{2\pi}\int_{-\pi}^{\pi}\frac{\epsilon^{-jkbRj(\phi)}}{R(\phi)}\epsilon^{-jn\phi}d\phi \quad (4)$$

Using equation 3 together with equation 2, it is seen that

$$K(\phi-\phi')=\sum_{-\infty}^{\infty}\alpha_n\epsilon^{jn(\phi-\phi')} \quad (5)$$

where

$$\alpha_n=\alpha_{-n}=kb\left\{\frac{K_{n+1}+K_{n-1}}{2}\right\}-\frac{n^2}{kb}K_n \quad (6)$$

Inserting expression 5 into integral equation 1 yields

$$V\delta(\phi)=\frac{j\zeta_0}{4\pi}\sum_{-\infty}^{\infty}\alpha_n\int_{-\pi}^{\pi}\epsilon^{jn(\phi-\phi')}I(\phi')d\phi' \quad (7)$$

After expanding $I(\phi)$ into a Fourier series

$$I(\phi)=\sum_{-\infty}^{\infty}I_n\epsilon^{jn\phi};\quad I_n=\frac{1}{2\pi}\int_{-\pi}^{\pi}I(\phi)\epsilon^{-jn\phi}d\phi \quad (8)$$

it can be seen that equation 7 reduces to the following

$$V\delta(\phi)=\frac{j\zeta_0}{2}\sum_{-\infty}^{\infty}\alpha_nI_n\epsilon^{jn\phi}$$

Hence

$$I_n=\frac{1}{j\pi\zeta_0\alpha_n}\int_{-\pi}^{\pi}\epsilon^{-jn\phi}V\delta(\phi)d\phi=\frac{V}{j\pi\zeta_0\alpha_n}$$

Inserting this result into equation 8 yields

$$I(\phi)=\frac{V}{j\pi\zeta_0}\sum_{-\infty}^{\infty}\frac{\epsilon^{jn\phi}}{\alpha_n}=\frac{V}{j\pi\zeta_0}\times\left(\frac{1}{\alpha_0}+2\sum_{1}^{\infty}\frac{\cos n\phi}{\alpha_n}\right) \quad (9)$$

From this, the impedance of the antenna Z is found to be

$$Z=\frac{V}{I(0)}=j\pi\zeta_0\left(\frac{1}{\alpha_0}+2\sum_{1}^{\infty}\frac{1}{\alpha_n}\right)^{-1} \quad (10)$$

These results, equations 9 and 10, obtained by Hallén, constitute a formal solution of the loop antenna. From them the transmitting pattern and by reciprocity the receiving pattern can be obtained. However, in order to make them useful, some way must be found to evaluate the series numerically.

It can be shown that these equations, 9 and 10, are in agreement with the theory of small loops. If equation 4 is used and the explicit evaluation of K_n given in Appendix III, it is readily shown that, for loops small in comparison to the wave length, the current is nearly a constant, independent of ϕ and

$$kb\ll 1,\ Z\cong j\pi\zeta_0\alpha_0=j\pi\zeta_0kbK_1$$

$$\cong\frac{\pi\zeta_0}{6}k^4b^4+j\pi\zeta_0kb\left(\ln\frac{8b}{a}-2\right)$$

This is the usual equation for the resistance and reactance of a small loop.

The Fourier Series

It is apparent from the preceding derivation that the usefulness of this method of solution depends on the evaluation of the series

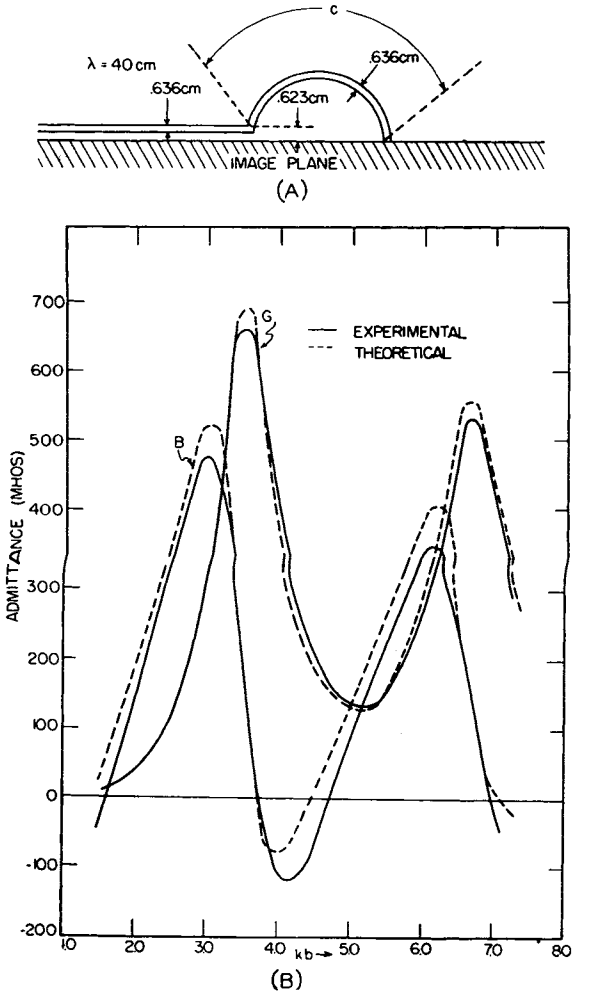

Fig. 2. A—Experimental dimensions. B—Impedance of loop antenna

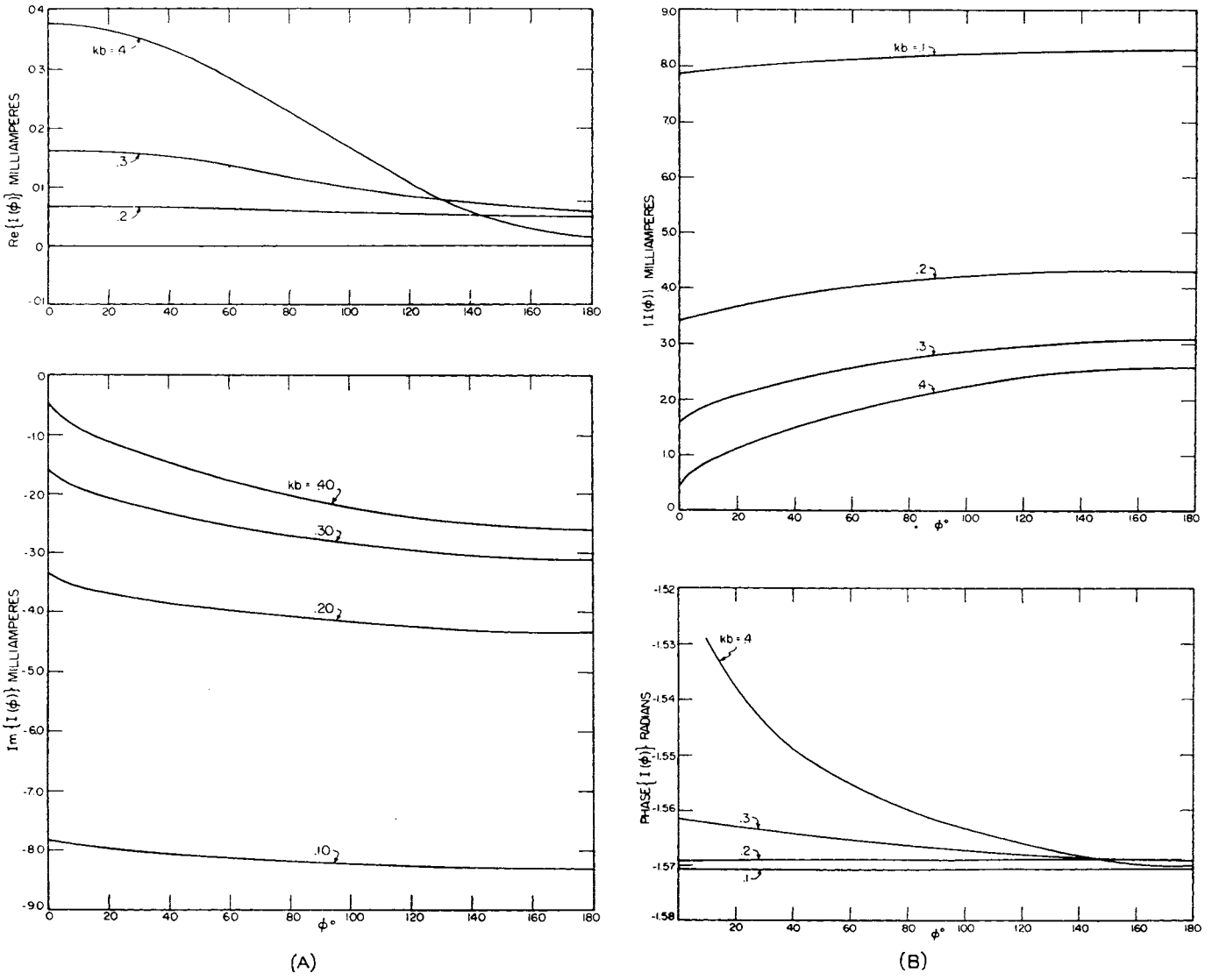

Fig. 3. A—Real and imaginary components of current distribution on small loop antennas; B—Magnitude and phase of current distribution on small loop antennas. In each case $\Omega = 2 \ln (2\pi b/a) = 10$

$$I(\phi) = \frac{jV}{\pi\zeta_0}\left(\frac{1}{\alpha_0} + 2\sum_{1}^{\infty}\frac{\cos n\phi}{\alpha_n}\right) \tag{11}$$

Hallén proved that, for large n, the coefficients approach asymptotically the value.

$$\alpha_n \cong\cong -\frac{n^2}{\pi kb}\left\{\ln\frac{2b}{a} - \gamma - \ln n\right\}$$

where $\gamma(=0.5772)$ is Euler's constant. It is apparent that α_n becomes extremely small for values of n such that

$$n \cong\cong n_0 = \frac{2b}{a}\epsilon^{-\gamma}$$

Hence the series 11 has a "singularity" near $n \cong\cong n_0$. From this fact Hallén concluded that the series 11 could only be used in an "asymptotic" fashion, i.e., it must converge satisfactorily by $r \cong\cong \frac{n_0}{2}$ since, after this, the value of the individual terms begin increasing in magnitude. This restriction meant that the series solution 11 was only useful for kb small or b/a very large. Even with this limitation the summation of $n_0/2$ terms of this series in a formidable task and, at best, yields relatively inaccurate results because of the "singularity."

It must be remembered at this point that current is both bounded and continuous (for physical reasons) and hence the series 11 must converge. When this point of view is adopted, the problem becomes one of treating Hallén's "singularity" in a more rigorous fashion.

A derivation of the value of αn is given in Appendix III, which is essentially identical to that of Hallén's, but which includes the dominant complex term as well. The result for large n is given as follows

$$\alpha_n \sim \frac{1}{\pi}\left(kb - \frac{n^2}{kb}\right)\left(\ln n_0 - \ln n - j\times\frac{(kb)^{2n+1}}{\Gamma(2n+2)}\right) \quad \begin{matrix} n > kb \\ n \gg 1 \end{matrix} \tag{12}$$

where $n_0 = \frac{2b}{a}\epsilon^{-\gamma}$

It is apparent that the inclusion of the rather negligible complex term in equation 12 cannot alter significantly the sum of the resulting series. However, with its inclusion α_n is never equal to zero. This fact will be used subsequently to permit a replacement of the series by an integral.

The following work will be restricted to loops in which $kb < 2.5$, i.e., the circumference of the loop is less than $2^1/_2$ wave lengths. (The derivation can readily be modified to include values of kb larger than 2.5 if desired.) Almost all loop antennas of practical interest are contained

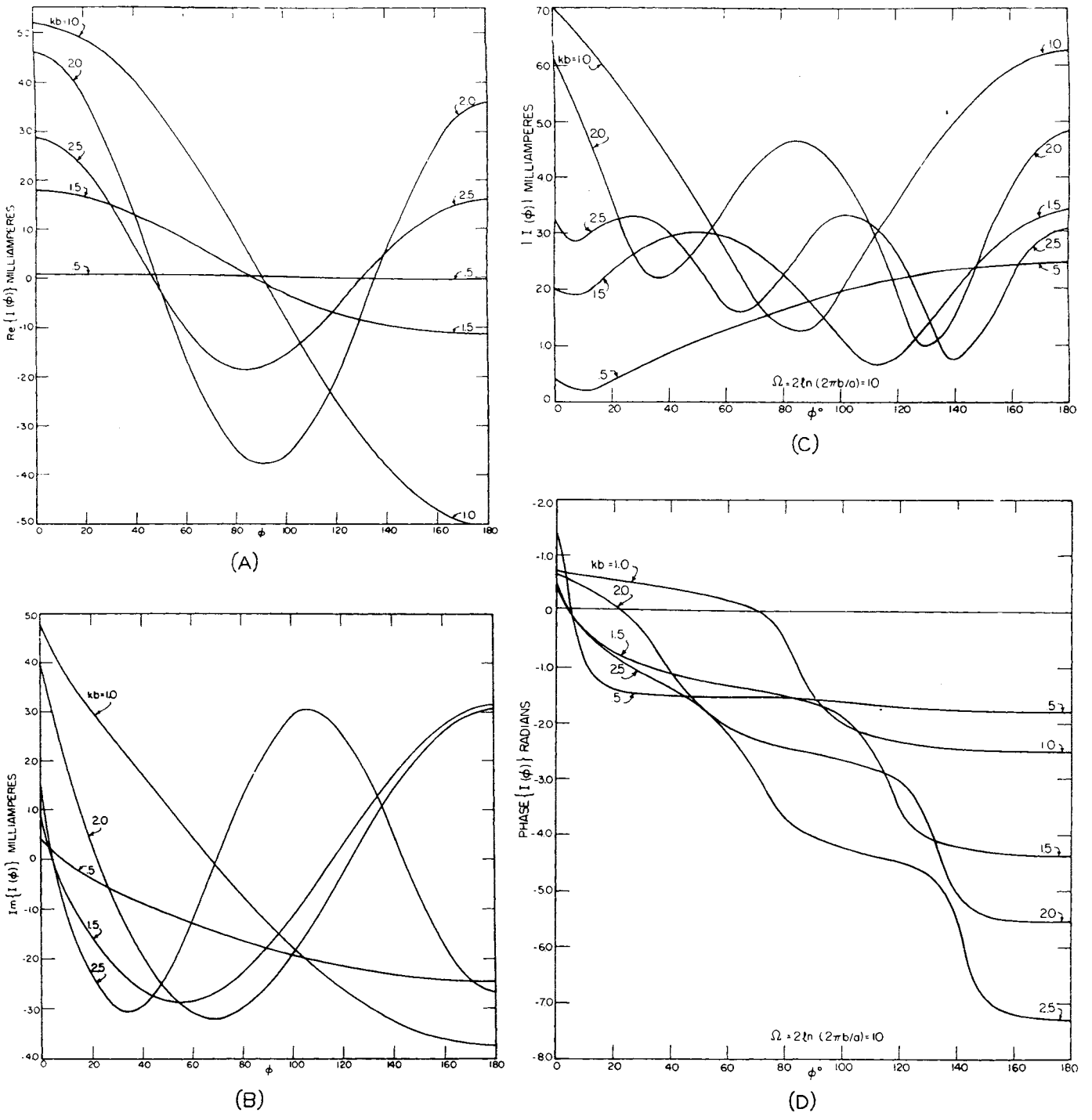

Fig. 4. A—Real part of current distribution on loop antennas. B—Imaginary component of current distribution on loop antennas. C—Magnitude of current distribution on loop antennas. D—Phase of current distribution on loop antennas. In each case $\Omega=10$

in this range. The series 11 can then be written in the form

$$I(\phi)=\frac{V}{j\pi\zeta_0}\left(\frac{1}{\alpha_0}+2\sum_{1}^{4}\frac{\cos n\phi}{\alpha_n}+\psi(\phi)\right) \quad (13)$$

where

$$\psi(\phi)=2\sum_{5}^{\infty}\frac{\cos n\phi}{\alpha_n}$$

The procedure to be used will sum the first five terms of the series explicitly, and replace the remainder of series $\psi(\phi)$ by an integral.

Now, it can be shown by an insertion of numerical values that for $kb\leqq 2.5$ and $n\geqq 5$, the value of α_n differs negligibly from the asymptotic value given by equation 12. Hence, to an excellent approximation

$$\psi(\theta)=-2\pi kb\sum_{5}^{\infty}\times$$

$$\frac{\cos n\phi}{(n^2-k^2b^2)[\ln n_0-\ln n-j(kb)^{2n+1}/\Gamma(2n+2)]} \quad (14)$$

The series 14 will now be replaced by an integral. The equation to be used is

$$\sum_{N}^{\infty}a_n=\int_{N-1/2}^{\infty}a_x dx+$$

$$\sum_{0}^{\infty}c_n\left[\frac{d^{2n+1}}{dx^{2n+1}}a_x\right]_{x=N-1/2} \quad (15)$$

Table I. Impedance of Loop Antennas as a Function of Frequency

$\Omega=8$, $2\pi b/a=54.60$. $\Omega=9$, $2\pi b/a=90.02$

R	X	G×10³	B×10³	kb	R	X	G×10³	B×10³
0.0048	43.57	0.0025	−22.95	0.05	0.0046	51.99	0.0017	−19.23
0.0402	88.77	0.0052	−11.36	0.10	0.0392	107.4	0.0034	−9.311
0.1533	140.5	0.0078	−7.119	0.15	0.1538	172.0	0.0052	−5.814
0.5939	205.7	0.0140	−4.860	0.20	0.5917	252.2	0.0093	−3.954
1.742	293.1	0.0203	−3.412	0.25	1.756	360.6	0.0135	−2.773
6.143	427.4	0.0336	−2.339	0.30	6.327	529.1	0.0226	−1.890
23.72	675.2	0.0520	−1.479	0.35	25.57	853.2	0.0351	−1.171
140.1	1344.0	0.0767	−0.7361	0.40	162.5	1776.0	0.0518	−0.5662
7972.7	2189.8	0.1172	−0.0322	0.45	1188.0	−3119.4	0.0796	0.0209
502.2	−1677.8	0.1638	0.5471	0.50	415.0	−1887.9	0.1111	0.5054
169.0	−824.4	0.2387	1.164	0.55	154.3	−962.0	0.1625	1.013
106.6	−544.1	0.3469	1.770	0.60	99.68	−639.4	0.2380	1.527
84.56	−400.2	0.5054	2.392	0.65	80.23	−471.9	0.3502	2.060
73.74	−311.8	0.7357	3.028	0.70	72.58	−367.1	0.5183	2.622
72.87	−250.3	1.072	3.683	0.75	70.48	−293.3	0.7744	3.223
73.28	−204.4	1.554	4.335	0.80	71.62	−237.5	1.164	3.860
76.02	−168.4	2.227	4.934	0.85	75.22	−192.8	1.757	4.502
80.72	−141.4	3.117	5.376	0.90	81.00	−155.6	2.633	5.057
87.59	−115.5	4.193	5.531	0.95	89.08	−122.7	3.874	5.337
94.81	−94.30	5.302	5.274	1.00	98.94	−95.22	5.247	5.050
104.4	−77.20	6.193	4.579	1.05	111.8	−70.25	6.413	4.030
115.4	−63.08	6.672	3.648	1.10	127.6	−48.16	6.860	2.589
128.0	−52.23	6.696	2.732	1.15	147.1	−29.22	6.541	1.300
142.0	−44.54	6.412	2.011	1.20	171.2	−14.36	5.899	0.4866
157.4	−41.09	5.949	1.553	1.25	200.4	−5.427	4.986	0.1350
172.9	−41.89	5.462	1.323	1.30	234.0	−4.986	4.271	0.0910
188.1	−48.12	4.991	1.277	1.35	270.2	−17.55	3.686	0.2394
200.7	−60.73	4.565	1.382	1.40	302.2	−46.51	3.232	0.4975
207.4	−76.86	4.240	1.571	1.45	320.5	−91.53	2.885	0.8239
207.5	−95.54	3.977	1.831	1.50	315.5	−142.0	2.636	1.186
199.8	−113.3	3.788	2.148	1.55	287.5	−184.7	2.462	1.581
186.0	−126.1	3.684	2.497	1.60	247.0	−207.6	2.373	1.994
169.5	−132.7	3.657	2.864	1.65	206.3	−211.7	2.361	2.423
152.8	−133.1	3.722	3.242	1.70	172.5	−202.6	2.437	2.862
138.7	−128.9	3.869	3.595	1.75	147.8	−186.7	2.607	3.293
127.8	−121.6	4.106	3.909	1.80	130.9	−168.1	2.883	3.703
119.5	−112.6	4.415	4.158	1.85	121.7	−149.6	3.273	4.023
115.4	−104.2	4.775	4.310	1.90	114.6	−131.4	3.774	4.282
113.2	−95.82	5.146	4.356	1.95	114.8	−115.1	4.345	4.357
113.4	−88.39	5.485	4.275	2.00	117.0	−101.6	4.915	4.226
114.4	−82.18	5.766	4.142	2.05	121.7	−87.95	5.398	3.902
116.8	−77.20	5.958	3.938	2.10	128.8	−77.59	5.697	3.432
119.9	−73.74	6.050	3.720	2.15	137.4	−70.01	5.776	2.941
123.2	−71.84	5.056	3.531	2.20	148.0	−64.94	5.665	2.485
126.2	−71.22	6.001	3.385	2.25	159.1	−63.49	5.421	2.163
129.3	−71.99	5.903	3.286	2.30	170.4	−65.77	5.108	1.972
131.1	−73.82	5.792	3.263	2.35	180.0	−72.08	4.788	1.918
131.9	−76.29	5.681	3.286	2.40	186.8	−81.78	4.492	1.966
131.7	−79.05	5.581	3.349	2.45	190.6	−94.78	4.206	2.091
130.1	−81.71	5.512	3.461	2.50	178.8	−106.4	4.031	2.284

where $c_0=1/24$, $c_1=-\dfrac{7}{2^4\times 360}$, etc.

This result, equation 15, is valid provided a_n is an analytic function of n in a region which includes the real axis for $n>N-1/2-\epsilon$. Results similar to equation 15 have been given by Gumowski[5] and others. It is essentially a modification of the Euler-McClaurin sum formula.

Using equation 15 in connection with equation 14 yields

$$\psi(\phi)=-2\pi kb\int_{4.5}^{\infty}\times \frac{\cos x\phi\,dx}{(x^2-k^2b^2)\left(\ln n_0-\ln x-j\dfrac{(kb)^{2n+1}}{\Gamma(2x+2)}\right)} \tag{16}$$

$$-\frac{2\pi kb}{24}\times\left[\frac{d}{dx}\frac{\cos x\phi}{(x^2-k^2b^2)\left(\ln n_0-\ln x-j\dfrac{(kb)^{2x+1}}{\Gamma(2x+2)}\right)}\right]_{x=4.5}-\ldots$$

This replacement of the series 15 by the integral is possible only because of the complex term, which makes the argument an analytic function of x along the real axis. Since $kb\leqq 2.5$, the first (and higher) derivative correction terms in equation 16 are small (less than 1 per cent) compared to $\psi(\phi)$ and can be ignored, since $\psi(\phi)$ is at best a minor part of $I(\phi)$ in equation 14. Hence,

$$\psi(\phi)=-2\pi kb\int_{4.5}^{\infty}\times \frac{\cos x\phi\,dx}{(x^2-k^2b^2)\left(\ln n_0-\ln x-j\dfrac{(kb)^{2x+1}}{\Gamma(2x+2)}\right)} \tag{17}$$

Next, it can readily be shown that the complex term in the integral of equation 17 can also be ignored. This yields

$$\psi(\phi)=-2\pi kb\int_{4.5}^{\infty}\frac{\cos x\phi\,dx}{(x^2-k^2b^2)(\ln n_0-\ln x)} \tag{18}$$

The integral in equation 18, which is to be interpreted in the principal-value sense, can be rewritten as follows

$$\psi(\phi)=\psi_1(\phi)+\psi_2(\phi) \tag{19A}$$

$$\psi_1(\phi)=-2\pi kb\int_{4.5}^{\infty}\frac{\cos x\phi}{\ln n_0-\ln x}\frac{dx}{x^2} \tag{19B}$$

$$\psi_2(\phi)=-2\pi kb\int_{4.5}^{\infty}\frac{\cos x\phi}{\ln n_0-\ln x}\times\frac{k^2b^2dx}{x^2(x^2-k^2b^2)} \tag{19C}$$

Since n_0 is quite large and $kb\leqq 2.5$, 19(C) becomes, to a satisfactory approximation

$$\psi_2(\phi)\cong\frac{-2\pi kb}{\ln n_0-\ln 4.5}\int_{4.5}^{\infty}\frac{k^2b^2\cos x\phi}{x^2(x^2-k^2b^2)}\,dx$$

$$\cong\frac{-2\pi k^3b^3}{\ln\left(\dfrac{n_0}{4.5}\right)}\int_{4.5}^{\infty}\frac{\cos x\phi}{x^4}\,dx$$

$$=-\frac{2\pi}{\ln\left(\dfrac{n_0}{4.5}\right)}\left(\frac{kb}{4.5}\right)^3J_2(\phi)$$

This integral, $J_2(\phi)$, can be evaluated explicitly in terms of sines, cosines, and integral sines.

With the use of these results, an explicit equation for the current distribution can be written as

$$I(\phi)=\frac{V}{j\pi\zeta_0}\left\{\frac{1}{\alpha_0}+2\sum_1^4\frac{\cos n\phi}{\alpha_n}-\frac{2\pi}{\ln\left(\dfrac{n_0}{4.5}\right)}\times\left[\left(\frac{kb}{4.5}\right)J_1(\phi)+\left(\frac{kb}{4.5}\right)^3J_2(\phi)\right]\right\} \tag{20}$$

where

$$J_1(\phi)=\int_1^{\infty}\frac{\ln\left(\dfrac{n_0}{4.5}\right)}{\ln\left(\dfrac{n_0}{4.5}\right)-\ln x}\frac{\cos(4.5\phi)}{x^2}\,dx \tag{21A}$$

$$J_2(\phi)=\int_1^{\infty}\frac{\cos(4.5x\phi)}{x^4}\,dx \tag{21B}$$

$n_0=\dfrac{2b}{a}\epsilon^{-\gamma}$ and explicit equations for the α_n are given in Appendix III.

Note that the $J_k(\phi)$ integrals have only appreciable values near $\phi=0$. (An asymptotic equation for them, when $\phi>1$, can readily be obtained.) They cannot be approximated satisfactorily by a sinusoid and they are a partial explanation of why approximate methods of dealing with the loop antenna do not yield good quantitative results.

The equation for the impedance of the loop antenna becomes

Table II. Impedance of Loop Antennas

$\Omega=10;\ 2\pi b/a=148.41.\quad \Omega=11;\ 2\pi b/a=244.69$

R	X	G×10³	B×10³	kb	R	X	G×10³	B×10³
0.0051	62.59	0.0013	−15.98	0.05	0.0047	72.24	0.0009	−13.84
0.0410	128.0	0.0025	−7.812	0.10	0.0411	147.0	0.0019	−6.803
0.1577	203.7	0.0038	−4.908	0.15	0.1532	233.9	0.0028	−4.275
0.5936	297.7	0.0067	−3.360	0.20	0.5991	342.7	0.0051	−2.918
1.777	425.8	0.0098	−2.348	0.25	1.744	488.8	0.0073	−2.046
6.355	624.4	0.0163	−1.601	0.30	6.263	713.6	0.0123	−1.401
25.47	1003.1	0.0253	−0.9963	0.35	24.43	1136.6	0.0189	−0.8793
159.7	2063.4	0.0373	−0.4818	0.40	149.1	2294.6	0.0282	−0.4339
1679.4	−3205.9	0.0571	0.0109	0.45	2203.2	5631.6	0.0430	−0.0107
468.8	−2250.5	0.0887	0.4258	0.50	479.5	−2768.6	0.0607	0.3505
156.6	−1142.6	0.1177	0.8590	0.55	167.7	−1360.8	0.0892	0.7238
100.7	−756.0	0.1731	1.300	0.60	106.0	−891.3	0.1316	1.106
80.95	−555.7	0.2567	1.762	0.65	84.42	−650.5	0.1962	1.512
73.25	−430.4	0.3842	2.258	0.70	75.87	−500.7	0.2959	1.952
71.23	−341.9	0.5841	2.803	0.75	73.50	−394.9	0.4556	2.448
72.60	−274.3	0.9018	3.407	0.80	74.78	−314.0	0.7175	3.013
76.57	−219.5	1.416	4.061	0.85	78.92	−248.3	1.162	3.657
82.99	−173.3	2.248	4.694	0.90	85.67	−192.1	1.937	4.342
91.97	−132.5	3.534	5.093	0.95	95.37	−141.5	3.274	4.859
103.7	−95.58	5.214	4.808	1.00	108.1	−95.57	5.192	4.591
119.2	−61.60	6.621	3.422	1.05	125.5	−51.61	6.816	2.804
138.9	−29.61	6.884	1.468	1.10	148.3	−8.771	6.720	0.3974
164.8	−12.50	6.067	0.0046	1.15	179.4	33.22	5.389	−0.9979
199.2	25.90	4.936	−0.6415	1.20	222.4	73.70	4.051	−1.342
244.4	45.67	3.954	−0.7390	1.25	282.8	109.6	3.074	−1.192
302.2	53.12	3.210	−0.5642	1.30	367.3	132.4	2.410	−0.8682
371.0	37.06	2.669	−0.2666	1.35	480.3	121.7	1.956	−0.4955
438.4	−16.75	2.278	0.0870	1.40	604.5	50.75	1.643	−0.1379
475.9	−109.9	1.995	0.4607	1.45	677.1	−122.7	1.430	0.2592
455.1	−214.2	1.799	0.8465	1.50	627.6	−308.0	1.284	0.6302
384.9	−286.2	1.673	1.244	1.55	491.3	−412.2	1.195	1.002
302.8	−309.7	1.614	1.651	1.60	355.3	−425.4	1.156	1.385
234.4	−299.8	1.619	2.070	1.65	260.3	−393.3	1.170	1.768
185.2	−274.2	1.692	2.504	1.70	198.2	−346.3	1.245	2.175
153.5	−242.6	1.863	2.944	1.75	162.4	−295.3	1.430	2.600
133.7	−211.3	2.139	3.380	1.80	138.1	−253.9	1.653	3.040
122.6	−181.7	2.551	3.781	1.85	126.3	−213.3	2.055	3.471
118.1	−154.5	3.122	4.086	1.90	122.1	−176.4	2.653	3.832
118.5	−129.8	3.836	4.202	1.95	124.0	−142.6	3.471	3.994
123.2	−107.5	4.610	4.019	2.00	130.5	−111.5	4.429	3.786
131.6	−87.41	5.272	3.500	2.05	142.1	−82.63	5.259	3.058
143.9	−69.91	5.625	2.732	2.10	159.2	−56.28	5.583	1.974
159.8	−55.64	5.580	1.942	2.15	182.5	−33.00	5.307	0.9598
179.6	−45.83	5.228	1.335	2.20	212.8	−15.14	4.678	0.3328
202.5	−41.74	4.737	0.9764	2.25	250.7	−4.160	3.988	0.0662
227.6	−45.36	4.226	0.8424	2.30	295.8	−6.389	3.380	0.0730
251.3	−58.68	3.774	0.8812	2.35	342.5	−27.26	2.901	0.2309
269.6	−81.82	3.397	1.031	2.40	379.2	−70.53	2.535	0.4715
277.5	−112.5	3.094	1.255	2.45	397.6	−132.8	2.263	0.7559
271.3	−144.3	2.873	1.528	2.50	381.6	−196.0	2.074	1.065

Table III. Impedance of Loop Antennas

$\Omega=12;\ 2\pi b/a=403.43$

kb	R	X	G×10³	B×10³
0.05	0.0053	81.46	0.0008	−12.28
0.10	0.0419	167.0	0.0015	−5.986
0.15	0.1548	265.3	0.0022	−3.769
0.20	0.5967	386.2	0.0040	−2.589
0.25	1.721	549.5	0.0057	−1.820
0.30	6.042	797.4	0.0095	−1.254
0.35	23.50	1255.6	0.0149	−0.7962
0.40	131.5	2446.6	0.0219	−0.4076
0.45	1465.2	14,782.6	0.0337	−0.0340
0.50	588.8	−3477.0	0.0474	0.2799
0.55	185.6	−1617.7	0.0700	0.6102
0.60	106.1	−1011.2	0.1033	0.9842
0.65	89.32	−754.6	0.1547	1.307
0.70	79.48	−576.3	0.2348	1.703
0.75	76.52	−451.4	0.3650	2.153
0.80	77.55	−356.1	0.5839	2.681
0.85	81.63	−278.4	0.9698	3.308
0.90	88.50	−211.6	1.682	4.022
0.95	98.43	−151.5	3.017	4.642
1.00	112.0	−95.32	5.178	4.406
1.05	130.5	−41.05	6.974	−2.194
1.10	155.3	13.30	6.393	−0.5478
1.15	190.7	67.58	4.660	−1.652
1.20	239.3	125.4	3.278	−1.718
1.25	312.5	181.6	2.392	−1.390
1.30	422.0	227.9	1.834	−0.9905
1.35	584.2	236.5	1.471	−0.5954
1.40	788.1	142.3	1.229	−0.2218
1.45	926.1	−116.0	1.063	0.1332
1.50	837.1	−419.6	0.9546	0.4785
1.55	610.9	−559.7	0.8899	0.8153
1.60	414.5	−854.2	0.8654	1.157
1.65	287.7	−493.0	0.8829	1.513
1.70	212.5	−422.5	0.9503	1.889
1.75	168.8	−356.6	1.085	2.291
1.80	144.0	−297.6	1.317	2.722
1.85	131.3	−245.3	1.696	3.168
1.90	123.8	−193.8	2.295	3.594
1.95	129.7	−154.6	3.185	5.796
2.00	137.6	−113.9	4.314	3.571
2.05	151.7	−75.20	5.292	2.623
2.10	172.7	−38.28	5.518	1.223
2.15	195.8	−36.02	4.941	0.0909
2.20	243.0	26.49	4.067	−0.4433
2.25	257.2	48.43	3.277	−0.5340
2.30	367.0	53.74	2.668	−0.3907
2.35	447.1	28.71	2.227	−0.1430
2.40	520.0	−39.84	1.912	0.1465
2.45	552.7	−148.0	1.688	0.4522
2.50	521.0	−259.2	1.538	0.7641

$$Z=j\pi\zeta_0\left\{\frac{1}{\alpha_0}+2\sum_1^4\frac{1}{\alpha_n}-\frac{2\pi}{\ln\left(\frac{n_0}{4.5}\right)}\times\left[\left(\frac{kb}{4.5}\right)J_1(0)+\left(\frac{kb}{4.5}\right)^3J_2(0)\right]\right\}^{-1} \quad (22)$$

This result, in connection with Appendix III, forms the basis for the impedance tables presented in Appendix I. The quantities $J_k(0)$ are explicitly given by the equation

$$J_1(0)=\frac{\ln\left(\frac{n_0}{4.5}\right)}{\left(\frac{n_0}{4.5}\right)}\int_{-\infty}^{\ln\left(\frac{n_0}{4.5}\right)}\frac{\epsilon^{+x}}{x}dx$$

$$J_2(0)=1/3$$

Results

The impedance of loop antennas for various values of b/a have been calculated with the use of equation 22. As a parameter, the quantity

$$\Omega=2\ln\frac{2\pi b}{a} \quad (23)$$

has been chosen. Note that $2\pi b/a=c/a$, where c is the circumference of the antenna. Hence equation 23 represents a definition analogous to that used for dipole antennas.

In Appendix I, values of the impedance are tabulated for $0\leqq kb\leqq 2.5$ and $\Omega=8$, 9, 10, 11, 12. They are also presented in graphic form. These impedances are useful for examining the operation of a loop antenna as a function of frequency. For laboratory purposes, however, it is sometimes convenient to have tables available appropriate to holding the frequency fixed and varying the size of the antenna. These tables, given in Appendix I, have been obtained by interpolation from the earlier tables.

It is perhaps worth while to comment on some of the more obvious features of these loop antenna impedances. As can be seen, the first antiresonance, occurring when the circumference of the loop approximates a half-wave-length, is extremely sharp. This well-known effect is easily explained by noting that a sufficiently small loop resembles closely a short-circuited quarter-wave-length transmission line and has a correspondingly sharp antiresonance.

Of equal interest is the rapid disappearance of resonances as the circumference of the antenna increases. Thus, for $\Omega\leqq 9$, a second resonance point does not even exist. If one compares these impedances with those for a dipole antenna, it is seen that the two are similar, both qualitatively and quantitatively, for $c>\lambda$. The prime difference is that the loop is essentially more capacitive (by about 130 ohms) than a dipole. This can be explained on the basis that changed surfaces are closer together on a loop than on a dipole. This shift in reactance level by 130 ohms permits the dipole to have several resonances and antiresonances, whereas, as noted previously, a moderately thick loop ($\Omega<9$) has essentially

(*Continued on page 615*)

Table IV. Input Impedance for ka Constant

a = 3/16 Inch at λ = 100 cm. a = 1/4 Inch at λ = 100 Cm. a = 5/16 Inch at λ = 100 Cm

Kb	R	X	R	X	R	X	Kb
0.05							0.05
0.10							0.10
0.15		149		133			0.15
0.20		244		217		196	0.20
0.25	2	385	2	357		313	0.25
0.30	7	625	6	526	6	500	0.30
0.35	25	999	27	908	23	801	0.35
0.40	172	2209	167	1986	169	1871	0.40
0.45	19992	−3998	15202	−5153	13535	−3981	0.45
0.50	376	−2320	408	−2251	410	−2094	0.50
0.55	170	−1348	152	−1200	129	−963	0.55
0.60	104	−905	103	−820	103	−767	0.60
0.65	85	−670	83	−613	81	−570	0.65
0.70	77	−525	75	−486	74	−465	0.70
0.75	75	−422	73	−391	72	−367	0.75
0.80	76	−342	75	−317	74	−298	0.80
0.85	81	−270	80	−255	78	−242	0.85
0.90	89	−210	87	−197	86	−188	0.90
0.95	98	−155	97	−150	96	−142	0.95
1.00	112	−102	110	−95	108	−95	1.00
1.05	132	−39	129	−45	126	−50	1.05
1.10	157	20	154	6	151	−3	1.10
1.15	195Ω	81	189	60	184	45	1.15
1.20	245(12.447)	152	238	118	231	95	1.20
1.25			311	178	299	145	1.25
1.30			426	229	402	186	1.30
1.35			589	244	547	191	1.35
1.40			836	167	739	118	1.40
1.45			988	−108	853	−119	1.45
1.50			918	−448	800	−400	1.50
1.55			689Ω	−613	600	−547	1.55
1.60			447(12.446)	−623	418	−553	1.60
1.65					289	−497	1.65
1.70					215	−434	1.70
1.75					170	−365	1.75
1.80					146	−309	1.80
1.85					134	−252	1.85
1.90					126	−200	1.90
1.95					132	−160	1.95
2.00					141Ω	−113	2.00
2.05					157(12.494)	−72	2.05

Table V. Input Impedance of Loop Antenna for ka Constant

a = 3/8 Inch at λ = 100 Cm. a = 1/2 Inch at λ = 100 Cm. a = 3/4 Inch at λ = 100 Cm

Kb	R	X	R	X	R	X	Kb
0.05							0.05
0.10							0.10
0.15							0.15
0.20							0.20
0.25	2	278					0.25
0.30	6	454	6	416			0.30
0.35	24	768	22	666			0.35
0.40	171	1738	146	1456			0.40
0.45	1216	−3160	1052		6772	2646	0.45
0.50	400	−1959	431	−1821	513	−1660	0.50
0.55	153	−1053	157	−954	166	−837	0.55
0.60	100	−716	95	−653	103	−570	0.60
0.65	81	−542	80	−495	82	−435	0.65
0.70	73	−430	73	−390	73	−345	0.70
0.75	72	−348	71	−318	71	−280	0.75
0.80	73	−283	72	−261	72	−232	0.80
0.85	78	−230	76	−215	76	−192	0.85
0.90	84	−182	83	−170	82	−158	0.90
0.95	94	−138	92	−133	90	−125	0.95
1.00	106	−95	104	−95	101	−95	1.00
1.05	124	−53	122	−60	115	−67	1.05
1.10	148	−12	142	−23	134	−40	1.10
1.15	179	33	171	13	158	−11	1.15
1.20	224	77	212	48	192	13	1.20
1.25	287	120	268	83	234	33	1.25
1.30	379	150	343	98	291	41	1.30
1.35	511	151	448	94	361	30	1.35
1.40	661	80	560	35	434	−15	1.40
1.45	774	−123	632	−116	487	−112	1.45
1.50	719	−353	617	−295	476	−224	1.50
1.55	552	−497	492	−410	402	−307	1.55
1.60	389	−508	356	−428	316	−337	1.60
1.65	280	−460	264	−404	243	−327	1.65
1.70	210	−405	202	−360	191	−300	1.70
1.75	168	−343	164	−310	159	−265	1.75
1.80	143	−291	140	−266	136	−232	1.80
1.85	133	−241	128	−225	125	−200	1.85
1.90	124	−193	122	−182	118	−168	1.90
1.95	130	−155	126	−150	122	−138	1.95
2.00	138	−112	134	−111	128	−110	2.00
2.05	153	−75	147	−79	139	−85	2.05
2.10	181	−35	170	−45	156	−60	2.10
2.15	211	5	193	−15	179	−40	2.15
2.20	250	40	235	15	209	−18	2.20
2.25	310	65	286	34	248	−5	2.25
2.30	395	80	353	39	294	−8	2.30
2.35	489	53	427	16	343	−27	2.35
2.40	598	−25	499	−42	387	−70	2.40
2.45	653*	−174	541	−148	409	−136	2.45
2.50			517†	−262	398‡	−201	2.50

* (Ω12.486).

† (Ω11.951).

‡ (Ω11.141).

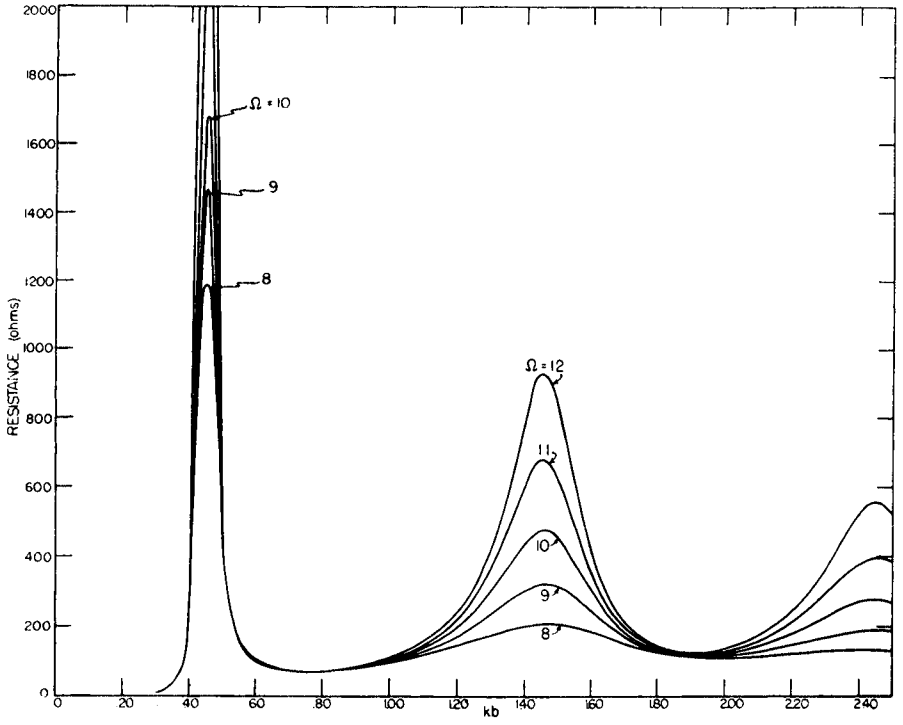

Fig. 5. Resistance of loop antennas as function of frequency

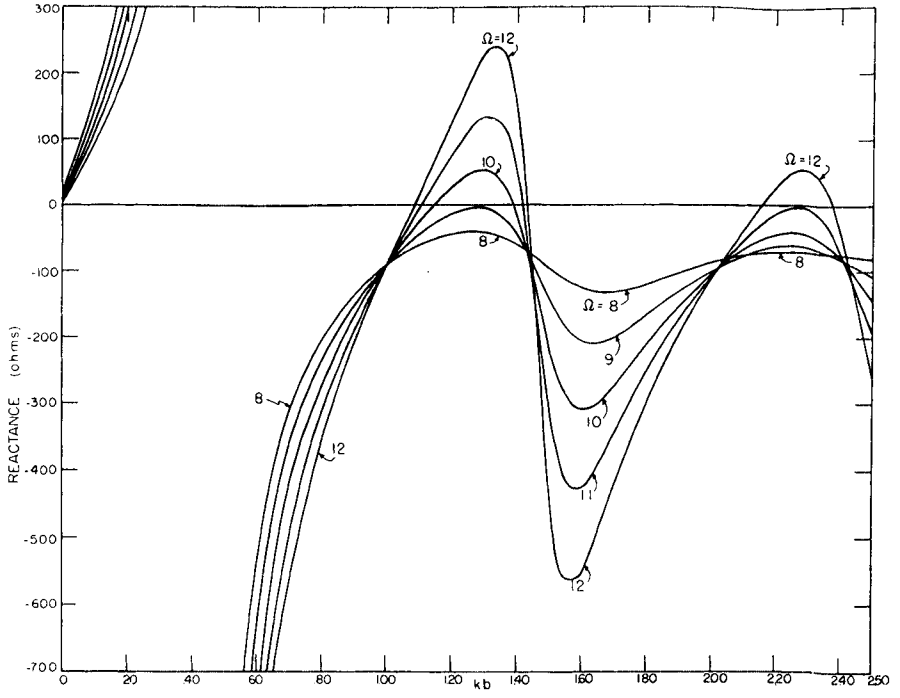

Fig. 6. Reactance of loop antennas as function of frequency

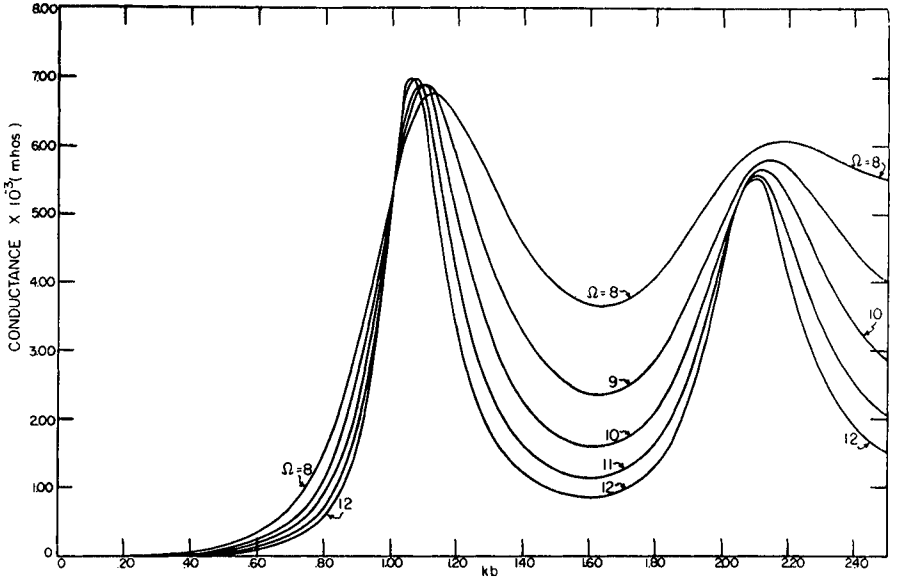

Fig. 7. Conductance of loop antennas as function of frequency

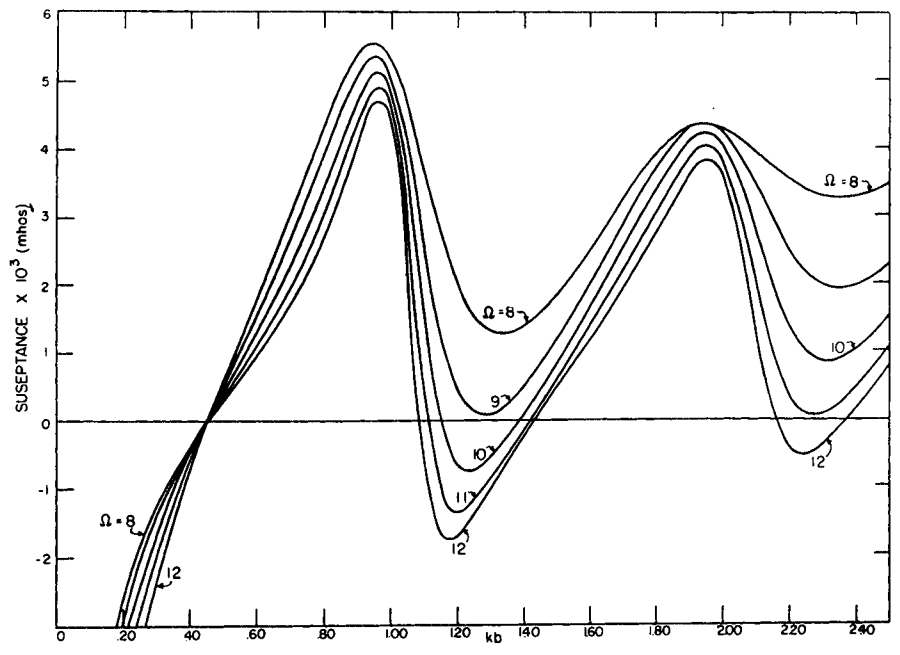

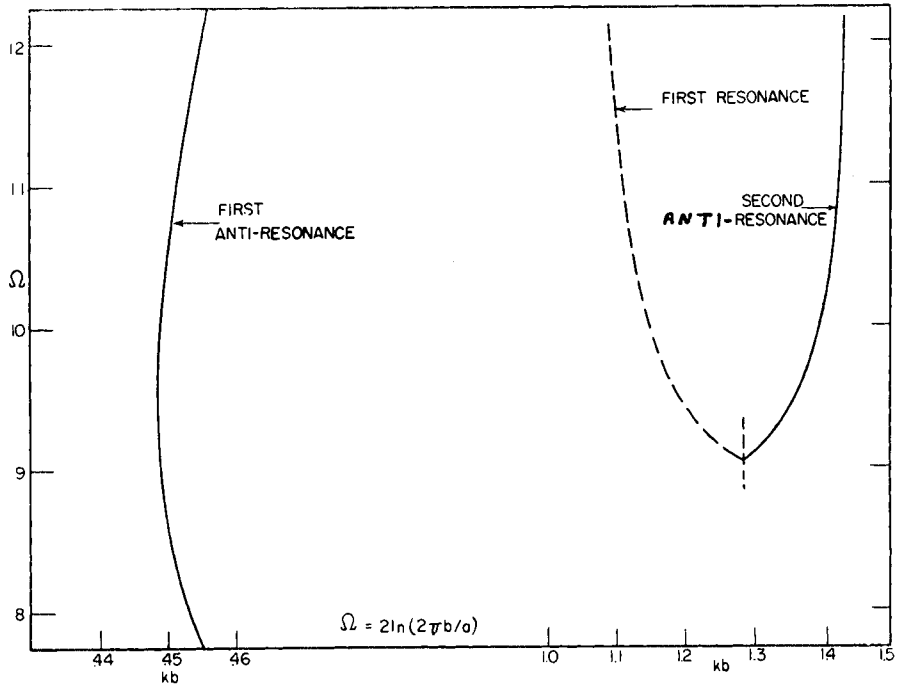

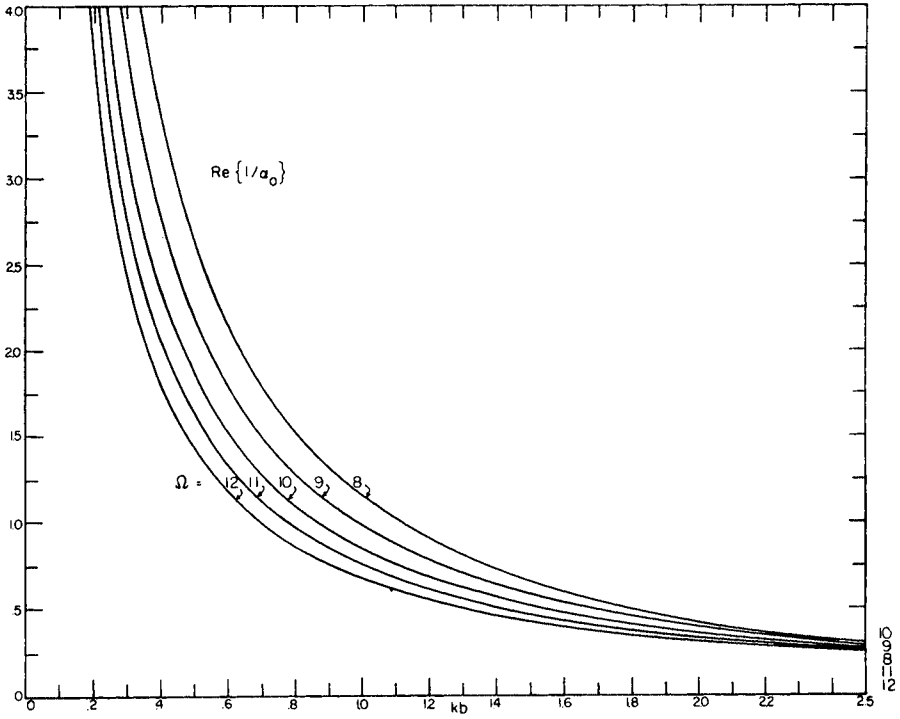

Fig. 8 (above left). Susceptance of loop antennas as function of frequency

Fig. 9 (left). Resonance and antiresonance points for loop antennas

Fig. 10 (above). Evaluation of equation 20: $R_e(1/\alpha_0)$; $\Omega = 8, 9, 10, 11, 12$, $kb \leqq 2.5$

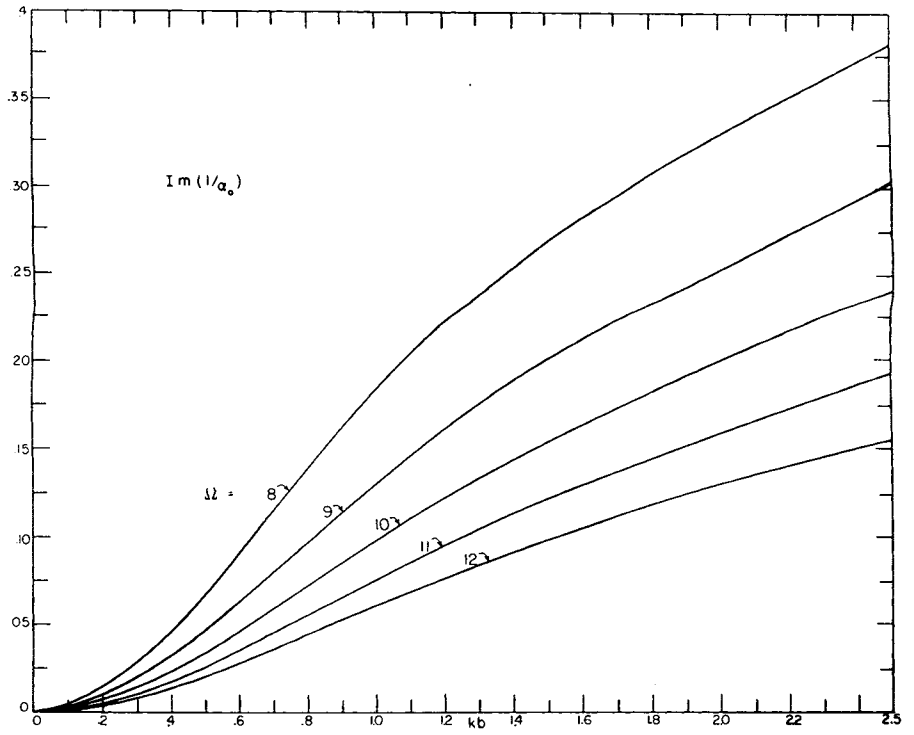

Fig. 11. Evaluation of equation 20: $I_m(1/\alpha_0)$; $\Omega = 8, 9, 10, 11, 12$, $kb \leq 2.5$

(Continued from page 611)

only one antiresonance. The resistance curves for the loop and dipole are very similar, with the resistance minima having almost identical values.

It is interesting to compare these theoretical loop impedances with some experimentally measured ones. Miss Phyllis Kennedy of Cruft Laboratory has measured some loop impedances, using a half-loop over an image plane, and driven by a 2-wire line. The explicit configuration is indicated in Fig. 2(A). One set of the admittances measured by Miss Kennedy appears in Fig. 2(B) together with the corresponding theoretical curves. The agreement between the theoretical and experimental curves is seen to be excellent. It is seen that the resistance peaks near resonance on the theoretical conductance curves are slightly higher than those on the experimental curve. This could have been anticipated, as ohmic losses of the loop were not taken into account in the theoretical solution. The two susceptance curves differ by a slight additive amount throughout the entire range. This can readily be attributed so the so-called end effect of the feeding line, which arises from coupling the fact that the transmission-line excitation differs from the "slice generator" used in the theoretical model. King[6] has calculated this end effect for a dipole antenna. The dominant correction term is a negative capacitance in shunt with the antenna. Quite obviously, the end correction for a loop antenna should be similar, even to the order of magnitude. If such an approximate correction is made to the susceptance curve of Fig. 2(B), this is changed in the right direction.

In Appendix II, values of the quantities $1/\alpha_k$ and the functions $J_k(\phi)$ are presented graphically to facilitate evaluation of the current distribution using equations 20 and 21. To obtain an idea of the type of current distributions on loop antennas, some were calculated for the explicit case of $\Omega = 10$. Because the $J_k(\phi)$ were evaluated by numerical integration, there exists a slight discrepancy between $I(0)$ and the admittance. Since the admittance values are more accurate, they were used in place of $I(0)$.

One of the classic assumptions in antenna literature is that a small loop has a constant current distribution. To examine the validity of the assumption, the actual current distributions were calculated for $\Omega = 10$ and $kb = 0.1$, 0.2, 0.3, and 0.4. These appear in Fig. 3. It is apparent that for the smallest loop, $kb = 0.1$, the current varies in magnitude by about 5 per cent and hence can be considered reasonably constant. For $kb = 0.2$, however, the variation is well over 10 per cent. On the basis of these results, one would be led to the conclusion that loops much larger than $kb = 0.2$ cannot be considered small.

To obtain an idea of how the distribu-

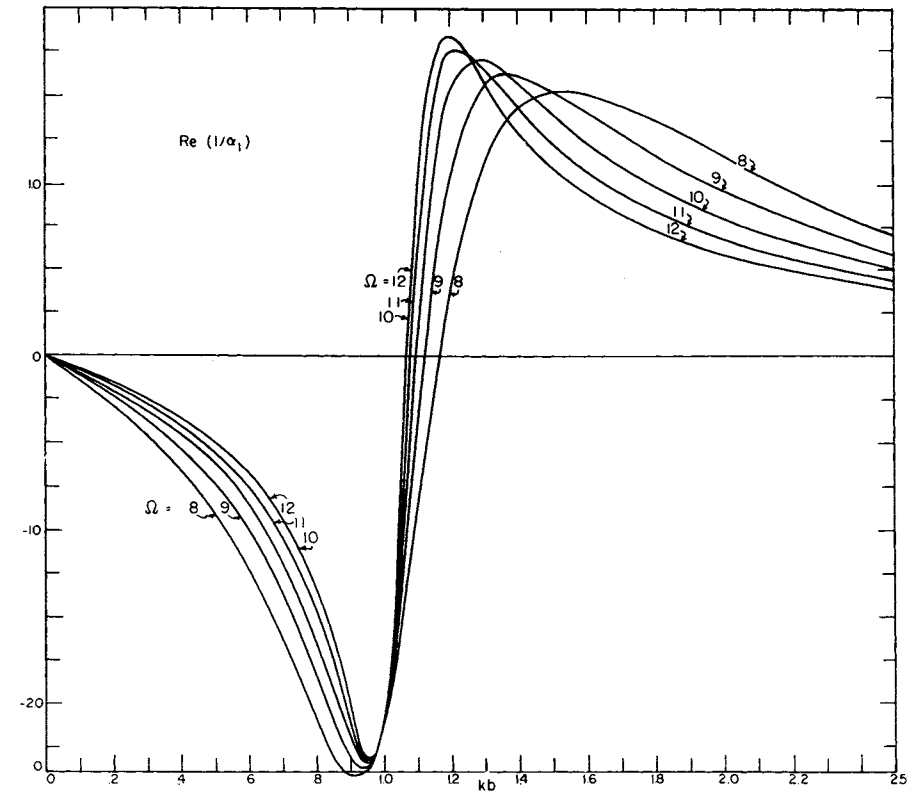

Fig. 12. Evaluation of equation 20: $R_e(1/\alpha_0)$; $\Omega = 8, 9, 10, 11, 12$, $kb \leq 2.5$

(Continued on page 618)

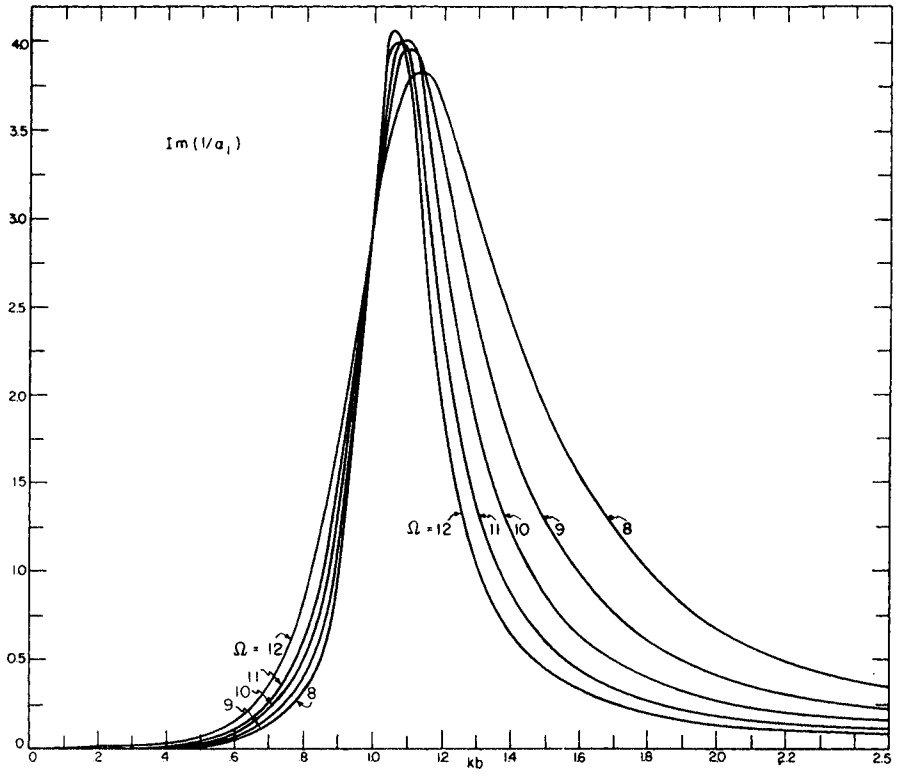

Fig. 13. Evaluation of equation 20: $I_m(1/\alpha_1)$, $\Omega = 8, 9, 10, 11, 12$, $kb \leqq 2.5$

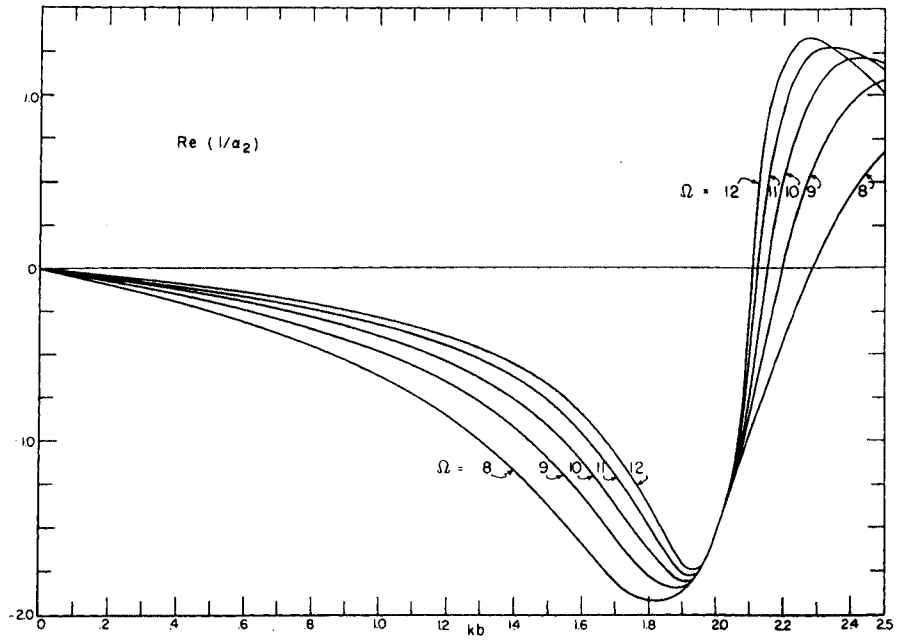

Fig. 14 (above right). Evaluation of equation 20: $R_e(1/\alpha_2)$, $\Omega = 8, 9, 10, 11, 12$, $kb \leqq 2.5$

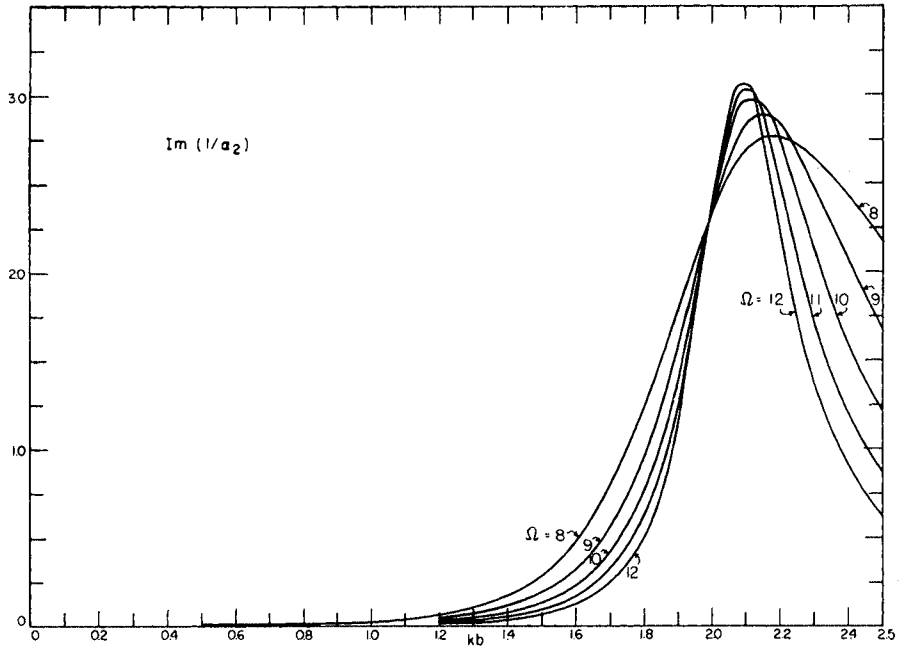

Fig. 15 (right). Evaluation of equation 20: $I_m(1/\alpha_2)$, $\Omega = 8, 9, 10, 11, 12$, $kb \leqq 2.5$

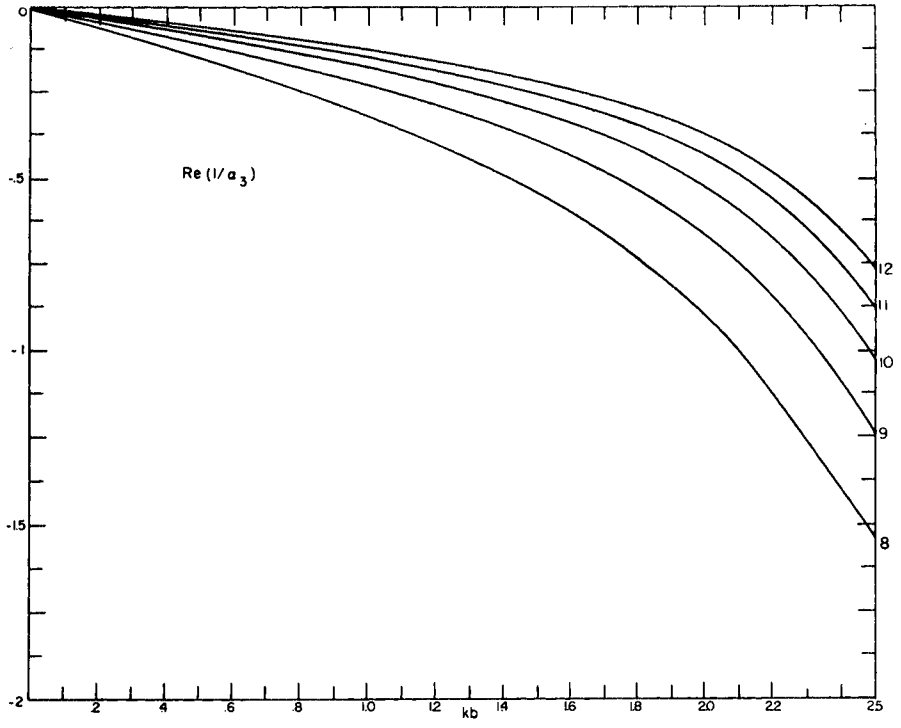

Fig. 16. Evaluation of equation 20: $R_e(1/\alpha_3)$; $\Omega = 8, 9, 10, 11, 12$, $kb \leqq 2.5$

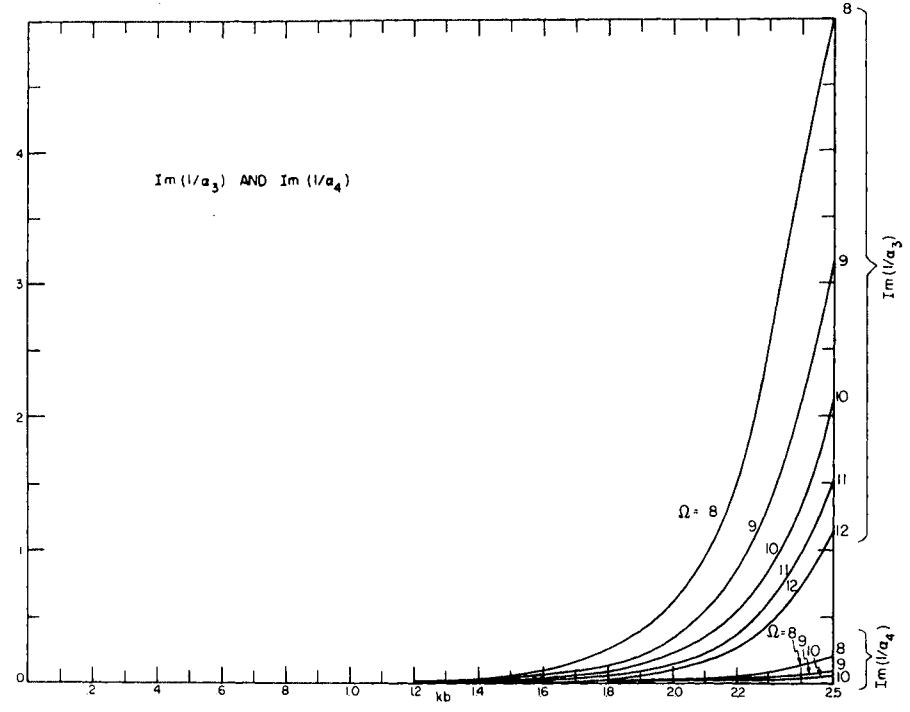

Fig. 17 (above right). Evaluation of equation 20: $I_m(1/\alpha_3)$ and $I_m(1/\alpha_4)$; $\Omega = 8, 9, 10, 11, 12$, $kb \leqq 2.5$

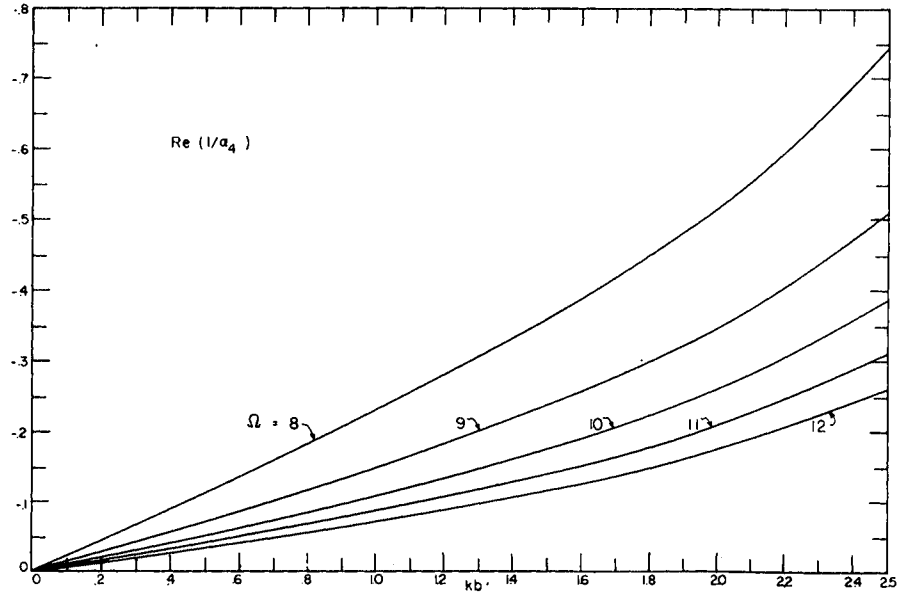

Fig. 18 (right). Evaluation of equation 20: $R_e(1/\alpha_4)$; $\Omega = 8, 9, 10, 11, 12$, $kb \leqq 2.5$

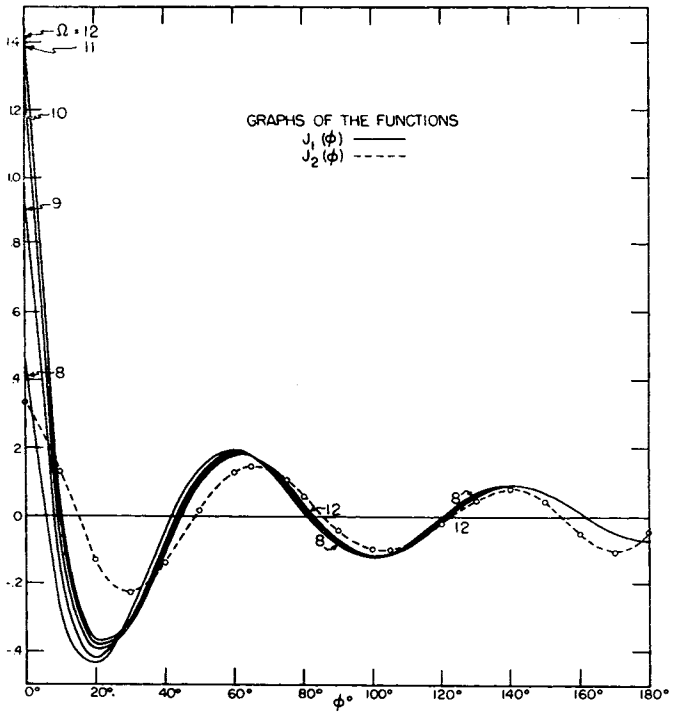

Fig. 19. Evaluation of equation 20: $J_1(\phi)$ and $J_2(\phi)$; $\Omega = 8, 9, 10, 11, 12$, $0 \leqq \phi \leqq \pi$

(*Continued from page 615*)

tion of current varies as the loop size increased, values of it were calculated for $\Omega = 10$ and $kb = 0.5$, 1.0, 1.5, 2.0, and 2.5. These results appear in Fig. 4. Perhaps the most noticeable feature in these curves appears in the plots of magnitude and phase for the larger values kb. For values of $\phi < 90$ degrees, it is apparent that the current distribution is beginning to approximate a traveling wave, in the sense that variations in the magnitude have been reduced and the phase is becoming linear. This is in agreement with the observation made in connection with the impedances, namely, that for larger kb the magnitude of the variation of the resistance is reduced.

Appendix I. Input Impedance of Loop Antennas

In Tables I through V impedances, $Z = R + jX$, are given in ohms and admittances, $Y = 1/Z = G + jB$, are given in mhos. The loop radius is designated by b and the loop wire radius by a. The ratio b/a is expressed in terms of the parameter $\Omega = \ln 2\pi b/a$. Note that $2\pi b = c$, the circumference of the loop, and $kb = 2\pi b/\lambda = c/\lambda$, where λ is the wave length. Thus kb is simply the circumference of the loop divided by the wave length.

The input impedance as a function of frequency is shown in graph form in Figs. 5 through 9 as follows:

Fig. 5: R versus kb for $\Omega = 8, 9, 10, 11, 12$; $kb \leqq 2.5$.
Fig. 6: X versus kb for $\Omega = 8, 9, 10, 11, 12$; $kb \leqq 2.5$.
Fig. 7: G versus kb for $\Omega = 8, 9, 10, 11, 12$; $kb \leqq 2.5$.
Fig. 8: B versus kb for $\Omega = 8, 9, 10, 11, 12$; $kb \leqq 2.5$.
Fig. 9: Locus of resonance and antiresonance points.

Tables I through III show input impedance and admittance as a function of frequency, as follows:

Table I: Z and Y versus kb for $\Omega = 8, 9$; $kb \leqq 2.5$.
Table II: Z and Y versus kb for $\Omega = 10, 11$; $kb \leqq 2.5$.
Table III: Z and Y versus kb for $\Omega = 12$; $kb \leqq 2.5$.

Tables IV and V show input impedance for ka constant, as follows:

Table IV: Z versus kb for $a = 3/16$ inch, 1/4 inch, 5/16 inch, at $\lambda = 100$ cm (centimeters).
Table V: Z versus kb for $a = 3/8$ inch, 1/2 inch, 3/4 inch, at $\lambda = 100$ cm.

Appendix II. Graphs to Facilitate Evaluation of Current Distribution on a Loop Antenna

The current distribution on a loop antenna is given explicitly by equation 20

$$I(\phi) = \frac{V}{j\pi\zeta_0}\left\{\frac{1}{\alpha_0} + 2\sum_1^4 \frac{\cos n\phi}{\alpha_n} - \frac{2\pi}{\ln \frac{n_0}{4.5}} \times \left[\left(\frac{kb}{4.5}\right)J_1(\phi) + \left(\frac{kb}{4.5}\right)^3 J_2(\phi)\right]\right\}_{kb \leqq 2.5} \quad (20)$$

where

V is the voltage driving the antenna
$\zeta_0 = 120$ ohms
a = radius of antenna wire
b = radius of antenna
$k = \omega/c = 2\pi/\lambda$

$$\ln(n_0/4.5) = \frac{\Omega}{2} - 3.226$$

$$\Omega = 2 \ln \frac{2\pi b}{a}$$

To facilitate evaluation of this equation, consult Figs. 10 through 19.

Appendix III. Evaluation of K_n

From equation 4 it is seen that

$$\Delta_n = K_{n+1} - K_n = \frac{1}{2\pi} \times \int_0^{2\pi} \frac{\epsilon^{-jkbR(\phi)}}{R(\phi)} [\epsilon^{j(n+1)\phi} - \epsilon^{jn\phi}] d\phi \quad n > 0$$

$$= \frac{1}{2\pi}\int_0^{2\pi} \frac{\epsilon^{-jkbR(\phi)}}{R(\phi)} \epsilon^{j\left(n+\frac{1}{2}\right)\phi} 2j \sin \phi/2 d\phi$$

The "thin-wire" approximation is that $k^2a^2 << 1$, $a^2 << b^2$. Neglecting terms of this order of magnitude yields

$$\Delta_n = \frac{1}{2\pi}\int_0^{2\pi} \frac{\epsilon^{-jkb \sin \phi/2}}{2 \sin \phi/2} \epsilon^{j\left(n+\frac{1}{2}\right)\phi} \times 2j \sin \phi/2 d\phi + \text{term of order } (a^2/b^2)$$

$$= \frac{j}{\pi}\int_0^{\pi} \epsilon^{-2jkb \sin \theta + j(2n+1)\theta} d\theta$$

$$= j[J_{2n+1}(2kb) - j\Omega_{2n+1}(2kb)]$$

where

$$J_{2n+1}(x) = \frac{1}{\pi}\int_0^{\pi} \sin(x \sin \theta - (2n+1)\theta) d\theta$$

is the Bessel function of order $2n+1$, and

$$\Omega_{2n+1}(x) = \frac{1}{\pi}\int_0^{\pi} \cos(x \sin \theta - (2n+1)\theta) d\theta$$

is the Lommel-Weber function of order $2n+1$, tabulated in Janke-Emde.

Thus, the foregoing result provides a recursion formula for K_n, i.e.,

$$\Delta_n = K_{n+1} - K_n = \Omega_{2n+1}(2kb) + jJ_{2n+1}(2kb), \quad n > 0$$

Therefore, all that remains to evaluate is K_0. This coefficient can be written as

$$K_0 = \frac{1}{2\pi}\int_0^{2\pi} \frac{\epsilon^{-jkbR(\phi)}}{R(\phi)} d\phi = \frac{1}{2\pi}\int_0^{2\pi} \frac{\epsilon^{-jkbR(\phi)} - 1}{R(\phi)} d\phi + \frac{1}{2\pi}\int_0^{2\pi} \frac{d\phi}{R(\phi)}$$

Now

$$\frac{1}{2\pi}\int_0^{2\pi} \frac{\epsilon^{-jkbR(\phi)} - 1}{R(\phi)} d\phi = \frac{1}{2\pi}\int_0^{2\pi} \frac{\epsilon^{-2jkb \sin \phi/2} - 1}{2 \sin \phi/2} d\phi + \text{term } 0(a^2/b^2)$$

$$= \int_0^{2kb} dx \left(-\frac{j}{\pi} \int_0^{\pi} \epsilon^{-jx \sin \phi} d\phi \right)$$

$$= -1/2 \int_0^{2kb} \Omega_0(x)dx - j/2 \int_0^{2kb} \times J_0(x)dx$$

It also can be shown[2]

$$\frac{1}{2\pi}\int_0^{2\pi} \frac{d\phi}{R(\phi)} = \frac{1}{\pi} \ln \frac{8b}{a} + \text{terms } 0(a^2/b^2)$$

So, to the order of approximation consistent with original integral equation

$$K_0 = \frac{1}{\pi} \ln \frac{8b}{a} - 1/2 \int_0^{2kb} \Omega_0(x)dx - j/2 \int_0^{2kb} J_0(x)dx$$

$$\Delta_n = K_{n+1} - K_n = \Omega_{2n+1}(2kb) + jJ_{2n+1}(2kb)$$

Another expression, useful for determining K_n for large n, can also be found. From the foregoing it is seen that

$$K_n = K_0 + \sum_0^{n-1} \Delta_n$$

Inserting the integral expressions for Δ_n yields

$$K_n = K_0 + \frac{j}{\pi} \sum_0^{n-1} \int_0^{\pi} \epsilon^{-2jkb \sin \phi + j(2n+1)\phi} d\phi$$

$$= K_0 + \frac{j}{\pi} \int_0^{\pi} \epsilon^{-2jkb \sin \phi} \left(\frac{e^{2jn\phi} - 1}{\sin \phi} \right) d\phi$$

Inserting the value for K_0

$$K_n = \frac{1}{\pi} \ln \frac{8b}{a} + \frac{1}{2\pi} \times \int_0^{\pi} (\epsilon^{-2jkb \sin \phi + 2jn\phi} - 1) \frac{d\phi}{\sin \phi}$$

$$= \frac{1}{\pi} \ln \frac{8b}{a} + \frac{1}{2\pi} \times \int_0^{\pi} (\epsilon^{-2jkb \sin \phi} - 1) \frac{\epsilon^{2jn\phi}}{\sin \phi} d\phi + \frac{1}{2\pi} \int_0^{\pi} (\epsilon^{2jn\phi} - 1) \frac{d\phi}{\sin \phi}$$

$$= \frac{1}{\pi} \ln \frac{8b}{a} - \frac{1}{2} \int_0^{2kb} [\Omega_{2n}(x) + jJ_{2n}(x)]dx - \frac{2}{\pi} \sum_0^{n-1} \frac{1}{2K+1}$$

This result can be used conveniently to determine the form of K_n for large N. For $n >> kb$, the integral is small, vanishing in the limit. Thus

$$n >> 1;\ n > kb,\ K_n \sim \left(\frac{1}{\pi} \ln \frac{8b}{a} - \frac{2}{\pi} \times \sum_0^{n-1} \frac{1}{2K+1} \right) - \frac{j}{2} \int_0^{2kb} J_{2n}(x)dx$$

Now, using Sterling's equation to evaluate the harmonic series, it can be shown that

$$\sum_0^{n-1} \frac{1}{2K+1} = \frac{\gamma}{2} + \frac{1}{2} \ln 4n,\ \gamma(=0.5772) \text{ is Eulers constant.}$$

Similarly, for $n > kb$

$$J_n(x) \cong \frac{1}{\Gamma(n+1)} \left(\frac{x}{2} \right)^n$$

So $K_n \sim \frac{1}{\pi} \left(\ln \frac{2b}{a} - \gamma - \ln n \right) - j \frac{(kb)^{n+1}}{\Gamma(2n+2)}$ $\begin{cases} n^2 \gg 1 \\ n > kb \end{cases}$

The Fourier coefficient α_n (4), can be written as

$$\alpha_n = \left(kb - \frac{n^2}{kb} \right) K_n + kb \left[\frac{\Delta_n - \Delta_n - 1}{2} \right]$$

Since Δ_n vanishes for large n, the asymptotic value of α_n is given by

$$\alpha_n \sim \left(kb - \frac{n^2}{kb} \right) \left[\frac{1}{\pi} \left(\ln \frac{2b}{a} - \gamma - \ln n \right) - j \frac{(kb)^{2n+1}}{\Gamma(2n+2)} \right] \quad \begin{cases} n^2 \gg 1 \\ n > kb \end{cases}$$

Finally (by simple insertion of numerical values), it can be shown that for $k \leqq 2.5$, and $n \geqq 5$, the asymptotic value of α_n as given differs negligibly from the correct value.

References

1. **H. C. Pocklington.** *Proceedings*, Cambridge Philosophical Society, London, England, vol. 9, 1897, p. 324.

2. **E. Hallén.** *Nova Acta Regiae Societatis Scientiarum Upsaliensis*, Uppsala, Sweden, series IV, vol. 2, no. 4, Nov. 1938.

3. **Tung Chang.** *Technical Report no. 16*, Cruft Laboratory, Harvard University, Cambridge, Mass, July, 1947.

4. ANTENNA THEORY AND PRACTICE (book), **S. A. Schelkunoff, H. T. Friis.** John Wiley & Sons, Inc., New York, N. Y., section 13.12, 1952.

5. SUMMATION OF SLOWLY CONVERGING SERIES, **I. Gumowski.** *Journal of Applied Physics*, New York, N. Y., vol. 24, 1953, p. 1068.

6. THEORY OF ANTENNAS DRIVEN FROM TWO-WIRE LINE, **R. King.** *Ibid.*, vol. 20, 1949, p. 832.

Diode-Shunting in Magnetic Amplifiers

J. L. LOWRANCE NONMEMBER AIEE

J. D. DOLAN NONMEMBER AIEE

IN THE self-saturating type of magnetic amplifier it is desirable to bias the saturable reactor to a particular point on its hysteresis loop. Higher gain and better linearity of the transfer function can be achieved in this manner. Shunt paths around the diodes of the magnetic amplifier afford a convenient means of biasing the saturable reactors.

The basic circuit examined in this report is a conventional full-wave, push-pull magnetic amplifier. An analysis is made of the bias currents in two different circuit arrangements. The feedback effects which are found in this type of circuit are discussed and the effective feedback factors for each circuit are determined.

Various methods of obtaining bias for the saturable reactors are shown in Fig. 1. Circuits 1 and 2 of Fig. 1 offer the advantage that fewer components are required.

Terms and Symbols

B = feedback coefficient
E = supply voltage
$\hat{E}$ = peak value of supply voltage
$\bar{E}$ = average value of supply voltage
H_θ = magnetization force required to saturate the magnetic core at angle θ of half-cycle, oersteds
I_D = current through dummy load resistor after both cores have saturated
I_D = average current through dummy load resistor after both cores have saturated
I_L = load current
$\bar{I}_L$ = average value of load current over half-cycle
I_n = net control current seen by amplifier
I_s = current from signal source
K_e = open loop voltage gain
K_e' = closed loop voltage gain
K_I = open loop current gain
K_I' = closed loop current gain
l_m = effective magnetic path length of core, centimeters
N_c = control-winding turns
N_{fb} = feedback-winding turns
N_g = gate-winding turns
R_c = control-winding resistance
R_d = dynamic foreward resistance of diode
R_D = dummy load resistor

Paper **56-749**, recommended by the AIEE Magnetic Amplifiers Committee and approved by the AIEE Committee on Technical Operations for presentation at the AIEE Summer and Pacific General Meeting, San Francisco, Calif., June 25–29, 1956. Manuscript submitted March 14, 1956; made available for printing May 8, 1956.

J. L. LOWRANCE and J. D. DOLAN are with the Bendix Aviation Corporation, South Bend, Ind.